COMMUNICATION

ChemComm
www.rsc.org/chemcomm

In situ detection of cytochrome c adsorption with single walled carbon nanotube device†

S. Boussaad,[a] N. J. Tao,[a] R. Zhang,[b] T. Hopson[b] and L. A. Nagahara[b]

[a] *Department of Electrical Engineering and Center for Solid State Electronics Research, Arizona State University, Tempe, Arizona, USA (85287). E-mail: Nongjian.Tao@asu.edu*

[b] *Physical Sciences Research Laboratories, Motorola Labs, Tempe, Arizona, USA (85284)*

Received (in Cambridge, UK) 11th March 2003, Accepted 1st May 2003
First published as an Advance Article on the web 20th May 2003

We report on the *in situ* detection of cytochrome c adsorption onto individual SWNT transistors *via* the changes in the electron transport properties of the transistors.

The ability to detect and study a single molecule[1–4] represents the ultimate challenge of biosensor development and analytical chemistry. Recent progress in the fabrication of nanostructured materials and devices, such as nanoparticles,[5] silicon nanowires,[6] metal nanowires[7,8] and carbon nanotubes[9,10] have opened new avenues for us to achieve this ability.

Single walled carbon nanotubes (SWNTs) are attractive for a wide range of applications, from nanoelectronics[11–13] and nanomechanics[14] to bioelectrochemistry.[15–17] Biomolecules, such as DNA[18] and proteins[19] have been immobilized on SWNTs and the biocompatible nature of SWNTs has been recently demonstrated,[15–17,20–22] which are significant steps toward biosensor applications. However, *in situ* detection of a small number of proteins *via* directly measuring the electron transport properties of a single SWNT has not been reported. In this letter we report on the detection of cytochrome c (cytc) adsorption onto individual SWNT transistors *via* the changes in the electron transport properties of the transistors. The adsorption of cytc induces a decrease in the conductance of the SWNT devices, corresponding to a few tens of molecules. We have studied the conductance *vs*. the electrochemical potential of the SWNT with respect to a reference electrode inserted in the solution, and observed a negative shift in the conductance *vs*. potential plot upon protein adsorption. From the shift, we have estimated the number of the adsorbed proteins, which is similar to that from the adsorption-induced conductance decrease. The results are supported by direct atomic force microscopy (AFM) images recorded before and after the protein adsorption.

The SWNT devices (Fig. 1) were prepared following a method similar to those reported in literature.[13,23] First, chemical vapor deposition (CVD) synthesis of individual nanotubes was performed on an array of catalyst paired-islands separated by 2 μm gap on a heavily doped Si wafer with 200 nm oxide layer. An array of gold electrodes (~300 nm thick) separated by 1 μm gap and aligned to overlap the catalyst pads was thermally evaporated. The devices were annealed (~600 °C) in a hydrogen-rich environment to ensure better contact between the nanotubes and the metallic electrodes. Before exposing the SWNTs to buffer and protein solutions, we characterized each of them by measuring the *I–V* at various gate voltages applied to the back of the chips. The characterization shows that while most of the SWNTs are p-type semiconducting, some are metallic. For semiconducting SWNTs, there is also a variation in the conductance, which allowed us to study the response of different SWNTs to the adsorption of the protein.

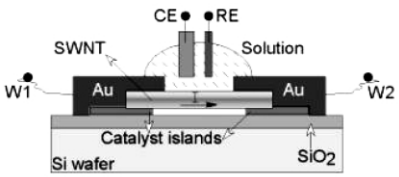

Fig. 1 Schematic illustration of a SWNT device.

The SWNTs were brought into contact with phosphate buffer (10 mM, pH = 7.0) using a solution cell. The leakage current due to the exposed gold electrodes is around 100 pA. We used Ag wire as a quasi-reference electrode and Pt wire as a counter electrode, and a custom-built bipotentiostat to control the electrochemical potential "gate" of each SWNT. After a stable conductance was obtained in the buffer solution, we introduced the protein solution into the cell. The protein solution, 200 μM cytc (Fluka) dissolved in phosphate buffer, was freshly prepared for each experiment. The redox activity of cytc was first verified electrochemically on highly ordered pyrolitic graphite (HOPG)[24] whose surface properties are similar to that of the nanotubes. The facile electron transfer between cytc and the substrate electrode indicates that the adsorbed protein orients its redox center, heme group, close to the electrode.

Figure 2a shows the conductance change for p-type and metallic nanotubes during the adsorption of cytc. Immediately after the protein (~10 μL) is introduced the conductance of the device begins to decrease and eventually reaches a stable value. The average time of the adsorption process lasts for a few mins, which is in good agreement with our previous study[24] of the adsorption of cytc on HOPG using real time AFM imaging. The decrease in conductance for the p-type SWNT reported here is expected for the positively charged protein adsorbed on the p-type SWNTs because it decreases the concentration of p-type carriers.

The adsorption-induced conductance decrease is observed for all semiconducting SWNTs (~30 devices), but the amount of decrease varies from one nanotube to another. For example,

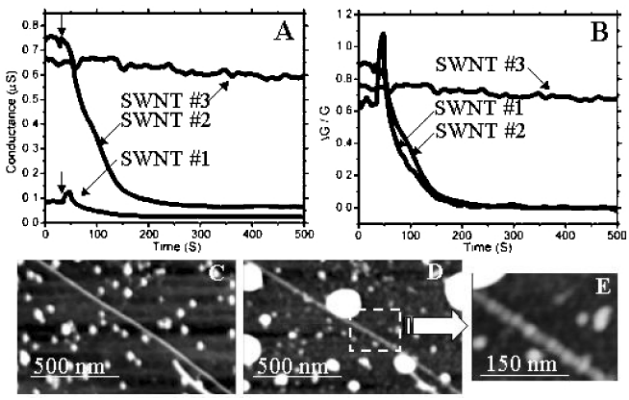

Fig. 2 (A) The conductance of p-type (1,2) and metallic (3) SWNTs simultaneously recorded as a function of time during the adsorption of the protein cytc. The arrow points to the start of the introduction of cytc into the buffer solution. (B) Plots of the relative change of conductance *vs* time. Tapping mode AFM images of a SWNT before (C) and after (D) the introduction of the protein solution. Image in E is the region outlined with a dashed rectangle in D.

† Electronic supplementary information (ESI) available: experimental details. See http://www.rsc.org/suppdata/cc/b3/b302681g/

DOI: 10.1039/b302681g

the conductance decrease for the SWNT shown in Fig. 2a (SWNT#2) is almost twice as much as the one shown in Fig. 2a (SWNT#1), although the difference in the relative change ($\Delta G/G$, Fig. 2b) between the two is small. We believe that this variation is mainly related to the electronic characteristics of the nanotubes, which determines the sensitivity of the conductance on the surface charge. We have measured the *I–V* characteristics *vs* the gate voltage (V_g) applied from the back of the chip for each nanotube before exposing to the solutions, and found a strong correlation between the amount of protein-induced conductance decrease and the dependence of the *I–V* characteristics on V_g. For metallic nanotubes, the *I–V* characteristic curves are insensitive to V_g and the adsorption of cytc induces no detectable change in the conductance (SWNT#3). For semiconducting nanotubes, the more sensitive is the dependence of the *I–V* curves on V_g, the greater is the protein-induced conductance decrease.

We have imaged the SWNTs before and after the adsorption of cytc with tapping-mode AFM. Figure 2c is an image obtained before exposing to cytc, which shows a rather smooth SWNT with some scattered residual photoresist particles on the chip. Figure 2d is an image of the same nanotube obtained after cytc adsorption, which reveals individual cytc on the nanotube (see Fig. 2e). By counting the number of cytc molecules on the nanotube, we found that the conductance decrease in Fig. 2a corresponds to the adsorption of 30–40 cytc molecules, which demonstrates the remarkable sensitivity of SWNTs for protein detection. This distribution of proteins on the surface of the nanotube observed by our AFM is very similar to that reported recently by Azamian *et al.*[16] for a cytc-functionalized SWNT. Unlike the conductance change that varies from one nanotube to another, the coverage of the adsorbed cytc as observed by AFM is similar for different nanotubes.

Like conventional field effect devices, the conductance of the SWNT device is sensitive to the surface charge, which can be used to estimate the number of adsorbed proteins independently from the AFM images. This task requires us to measure the conductance *vs* the electrochemical gate potential. Figure 3 shows the typical result of such a measurement in phosphate buffer (10 mM). The data were recorded by measuring the current through the nanotube at small fixed bias voltage (10 mV) applied between the two ends of the nanotube while the potential of the nanotube was swept with respect to the reference electrode inserted in the buffer solution. At positive potential, the conductance is small, but increases quickly as the potential decreases towards negative values. The dependence shown in Fig. 3 is expected for a p-type SWNT and is in agreement with recent results by other groups[23,25] From the conductance (G) *vs* potential (V) plot, we have estimated $\Delta G/\Delta V$ ($\sim 10^{-6}$ S V^{-1}), which allows us to relate charge change (ΔQ) to the conductance change (ΔG) according to:

$$\Delta Q = C\left(\frac{\Delta G}{\Delta V}\right)^{-1}\Delta G$$

where C is the capacitance, which is dominated by the quantum capacitance (4×10^{-10} F m^{-1}) of the SWNT.[23] For a 1 μm SWNT, the quantum capacitance is $\sim 4 \times 10^{-16}$ F. Using the above relation, the number of cytc molecules for a given conductance decrease can be determined if the charge per protein is known. The surface charge of cytc is well characterized and it is ~ +10e per protein at pH = 7.[26] For the adsorption-induced conductance plots shown in Fig. 2, we estimated that the number of cytc molecules is ~25, which is consistent with the AFM data.

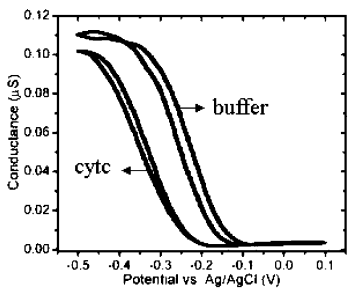

Fig. 3 A plot of the conductance of a p-SWNT as function of the electrochemical potential in phosphate buffer and 200 μM cytc in buffer.

As expected the adsorption of cytc causes a shift in the G *vs* V plot toward negative potentials. Note that the protein adsorption does not change the slope and the shape of the plot, which is consistent with the finding that the capacitance of the SWNTs is dominated by the quantum capacitance. The average shift is approximately 0.090 V. Using the above-mentioned capacitance, the corresponding charge change brought by the adsorbed molecules of cytc is ~ +200e. Therefore, the number of adsorbed cytc molecules on the SWNT is ~20. This is in agreement with the number of molecules estimated from the AFM images and the adsorption plots. Our results show that a small number of molecules of cytc can be detected by measuring the transport properties of the SWNTs.

Financial support (NJT) from DOE(DE-FG03-01ER45943) and EPA(R82962301) is greatly appreciated. We thank Ray Tsui (Motorola) and Xuilan Li (ASU) for help in device preparation.

Notes and references

1 S. Nie and S. R. Emroy, *Science*, 1997, **275**, 1102–1105.
2 H. P. Lu, L. Y. Xun and X. S. Xie, *Science*, 1998, **282**, 1877–1882.
3 F.-R. F. Fan and A. J. Bard, *Science*, 1995, **267**, 871–874.
4 F.-R. F. Fan, J. Kwak and A. J. Bard, *J. Am. Chem. Soc.*, 1996, **118**, 9669–9675.
5 L. C. Brousseau III, Q. Zhao, D. A. Shultz and D. L. Feldheim, *J. Am. Chem. Soc.*, 1998, **120**, 7645–7650.
6 Y. Cui, Q. Wei, H. Park and C. M. Lieber, *Science*, 2001, **293**, 1289–1292.
7 F. Favier, C. W. Erich, M. P. Zach, T. Benter and R. M. Penner, *Science*, 2001, **293**, 2227–2230.
8 C. Z. Li, H. X. He, A. Bogozi, J. S. Bunch and N. J. Tao, *Appl. Phys. Lett.*, 2000, **76**, 1333–1336.
9 J. Kong, N. R. Franklin, Zhou, M. G. Chapline, S. Peng, K. Cho and H. Dai, *Science*, 2000, **287**, 622–625.
10 P. G. Collins, K. Bradley, M. Ishigami and A. Zettll, *Science*, 2000, **287**, 1801–1804.
11 J. Appenzeller, R. Martel, V. Derycke, S. Radosavljević, S. Wind, D. Neumayer and Ph. Avouris, *Microelectron. Eng.*, 2002, **64**, 391–397.
12 S. J. Tans, A. R. M. Verschueren and C. Dekker, *Nature*, 1998, **393**, 49–52.
13 C. Zhou, J. Kong, E. Yenilmez and H. Dai, *Science*, 2000, **290**, 1552–1555.
14 A. Minett, J. Fràysse, G. Gang, G.-T. Kim and S. Roth, *Curr. Appl. Phys.*, 2002, **2**, 61–64.
15 J. J. Davis, R. J. Coles and A. O. Hill, *J. Electrochem. Chem.*, 1997, **440**, 279–282.
16 B. R. Azamian, J. J. Davis, K. S. Coleman, C. B. Bagshaw and M. L. H. Green, *J. Am. Chem. Soc.*, 2002, **124**, 12664–12665.
17 A. Guiseppi-Eli, C. Lei and R. H. Baughman, *Nanotechnology*, 2002, **13**, 559–564.
18 Z. Guo, P. J. Sadler and S. C. Tsang, *Adv. Mater.*, 1998, **10**, 701–703.
19 R. J. Chen, Y. Zhang, D. Wang and H. Dai, *J. Am. Chem. Soc.*, 2001, **123**, 3838–3839.
20 K. F. Fu, W. J. Huang, Y. Lin, D. H. Zhang, T. W. Hanks, A. M. Rao and Y. P. Sun, *J. Nanosci. Nanotechnol.*, 2002, **2**, 457–461.
21 J. J. Davis, M. L. H. Green, H. A. O. Hill, Y. C. Leung, P. J. Sadler, J. Sloan, A. V. Xavier and S. C. Tsang, *Inorg. Chim. Acta*, 1998, **272**, 261–266.
22 F. Balavoine, P. Schultz, C. Richard, V. Mallouh, T. W. Ebbesen and C. Mioskowski, *Angew. Chem. Int. Ed.*, 1999, **38**, 1912–1915.
23 S. Rosenblatt, Y. Yaish, J. Park, J. Gore, V. Sazonova and P. L. McEuen, *Nano letters*, 2002, **2**, 869–872.
24 S. Boussaad, N. J. Tao and R. Arechabaleta, *Chem. Phys. Lett.*, 1997, **280**, 397–403.
25 S. Kazaoui, N. Minami, N. Matsuda, H. Kataura and Y. Achiba, *Appl. Phys. Lett.*, 2001, **78**, 3433–3435.
26 G. R. Moore and G. W. Pettigrew, in *Cytochromes c: evolutionary, structural and physicochemical aspects* 1990 Springer-Verlag.